ENGINEERING PROPERTIES OF SCRAP TIRES USED IN GEOTECHNICAL APPLICATIONS

REPORT 95-1
FEBRUARY 1995

STATE OF VERMONT
AGENCY OF TRANSPORTATION
MATERIALS AND RESEARCH DIVISION

PATRICK J. GARAHAN, SECRETARY OF TRANSPORTATION
FRANK C. EVANS, DIRECTOR OF CONSRUCTION AND MAINTENANCE
ROBERT F. CAULEY, MATERIALS AND RESEARCH ENGINEER

Prepared By:

Christopher C. Benda, P.E.
Soils and Foundations Engineer

Reviewed By:

Robert Cauley

R.F. Cauley
Materials and Research Engineer

Date: FEB 22 1995

TECHNICAL REPORT STANDARD TITLE PAGE

1. Report No.	2. Government Accession No.	3. Recipient's Catalog No.
95-1		

4. Title and Subtitle	5. Report Date
Engineering Properties of Scrap Tires Used In Geotechnical Applications	FEB 1995
	6. Performing Organization Code

7. Author(s)	8. Performing Organization Report No.
Christopher C. Benda	95-1

9. Performing Organization Name and Address	10. Work Unit No.
Vermont Agency of Transportation 133 State Street - State Administration Building c/o Materials and Research Division Montpelier, Vermont 05633-5001	11. Contract or Grant No.
12. Sponsoring Agency Name and Address	13. Type of Report and Period Covered
Vermont Agency of Transportation	14. Sponsoring Agency Code

15. Supplementary Notes

16. Abstract

Waste tires are being generated in the United States at a startling rate and their disposal is an increasing environmental and economic concern. Scrap tires cut into chips have shown a great deal of potential as lightweight fill, retaining wall backfill and as a free draining medium in geotechnical and highway engineering applications.

Compression loading and unloading triaxial tests were conducted to determine the compressibility, shear strength and elastic characteristics of five processed scrap tire products having different gradations and particle shapes. Densities of the compacted tire scraps at an 8.0 psi confining pressure were between 42.3 and 47.6 pcf. At rest earth pressure coefficients varied between 0.30 and 0.50.

Compression loading tests revealed a minimum failure envelope of 30 degrees for all products at axial strains of 15 to 18 percent. Compression unloading tests yielded peak friction angles of 45 to 60 degrees at approximately 10 percent lateral strain.

Based on this and other research, it is recommended that the Vermont Agency of Transportation consider using tire chips where there is a need for lightweight fill, reduced lateral earth pressures or material with a large hydraulic conductivity. Recommendations for design and additional research are presented.

17. Key Words	18. Distribution Statement
Earth Work, Embankment, Materials, Tire Chips	Unrestricted

19. Security Classif. (of this report)	20. Security Classif. (of this page)	21. No. of Pages	22. Price
Unclassified	Unclassified	30	N/A

Form DOT F 1700.7 (8-69)

ENGINEERING PROPERTIES OF SCRAP TIRES USED IN GEOTECHNICAL APPLICATION

INTRODUCTION

The Environmental Protection Agency estimates that over 242 million scrap tires are generated each year in the United States and another 2 to 3 billion waste tires currently exist in stockpiles or in tire dumps. As of 1991, 78% of scrap tires were stockpiled, landfilled or illegally dumped and only 6% were being recycled. It is estimated that each person discards one tire every year in this country alone (*1*).

Stimulated by the need to reduce this waste stream and by recent legislation at the state and federal levels, alternate disposal, recycling and reuse options for scrap tires are being revisited by the highway industry (*2*). Preliminary testing conducted on scrap tires cut into chips indicates tire chips have properties which make them desirable for use as lightweight fill in highway embankments and backfill behind retaining walls (*3*). The tire chips are durable, consist primarily of coarse grained particles and have a specific gravity below 1.3. They are free draining and the compacted density is approximately one-third that of conventional granular material. The resulting lateral earth pressure in retaining wall applications and vertical stresses causing settlements in soft soil would be significantly reduced if the tire chips were used as fill.

The Vermont Agency of Transportation (VAOT) has used or has considered using tire chips as a substitute for free draining granular material in underdrain applications, as lightweight fill to reduce downdrag on piles founded in compressible soils and to flatten slopes to eliminate the need for guardrail. Other projects include using tire chips as a thermal insulation layer to reduce frost penetration, in embankments to remediate slope stability problems and as retaining wall backfill to lower horizontal earth pressures (*4*).

Incorporating tire chips into roadway embankments and retaining structures requires knowledge of how the material will perform and of engineering properties from which to safely and reliably design these transportation facilities. Properties, including permeability, shear strength, density at various compactive efforts, lateral earth pressure coefficients and compressibility of the tires chips have been studied to various degrees at the University of Maine (*5,6*). This work provides the foundation on which the research presented herein is based.

Field observations of tire chip placement in stockpiles and fills suggests the shear strength of this material is higher than the results of laboratory shear tests conducted previously would indicate. End-dumped tire chips and open cuts in stockpiles stand vertically for extended periods without collapsing indicating the actual shear strength may be higher than that measured in the laboratory using direct shear testing techniques. The shear strength determined in earlier testing using a direct shear apparatus on three sources of tire chips resulted in a range of friction angles, ϕ, of 19 to 26 degrees and cohesion intercepts of 90 to 240 psf. Failure was assumed to occur at a horizontal strain equal to 10 percent of the shear box length (*6*).

The purpose of this research was to determine what effect particle size, shape and distribution have on the shear strength of this material and what friction angle values are appropriate for use in design. In order to more closely model the loading expected under field conditions, it was decided to use a triaxial compression testing apparatus to perform the analysis.

MATERIALS

Gradation and Particle Shape

A comparison was made of five processed scrap tire products having particle size distributions as shown in Figure 1. Source, maximum size, principal particle shape and uniformity coefficients, C_u, are given in Table I.

TABLE I, Product Source and Description

PRODUCT	SOURCE	MAXIMUM SIZE	PARTICLE SHAPE	C_u
1	Palmer Shredding Ferrisburg, Vt.	1.5"	Flaky	1.67
2	Palmer Shredding Ferrisburg, Vt.	0.75"	Angular	1.53
3	Palmer Shredding Ferrisburg, Vt.	0.375"	Elongated	2.53
4	RCI Hicksville, NY.	0.375"	Irregular	3.28
5	Baker Rubber Chambersburg, Pa.	No. 10	Angular	1.45

Product 1 most closely represents the type of material that would be used in field applications from a size and particle shape standpoint. Tire scraps used by the U.S. Army Cold Regions Research and Engineering Laboratory (CRREL) and by VAOT in gravel roads consisted primarily of material finer than the 3 inch sieve and coarser than the No. 4 sieve (*4,7*). Product 2 was less flaky than product 1 and tended towards a more cubical particle shape, mainly because the top size was limited to 0.75 inches. Product

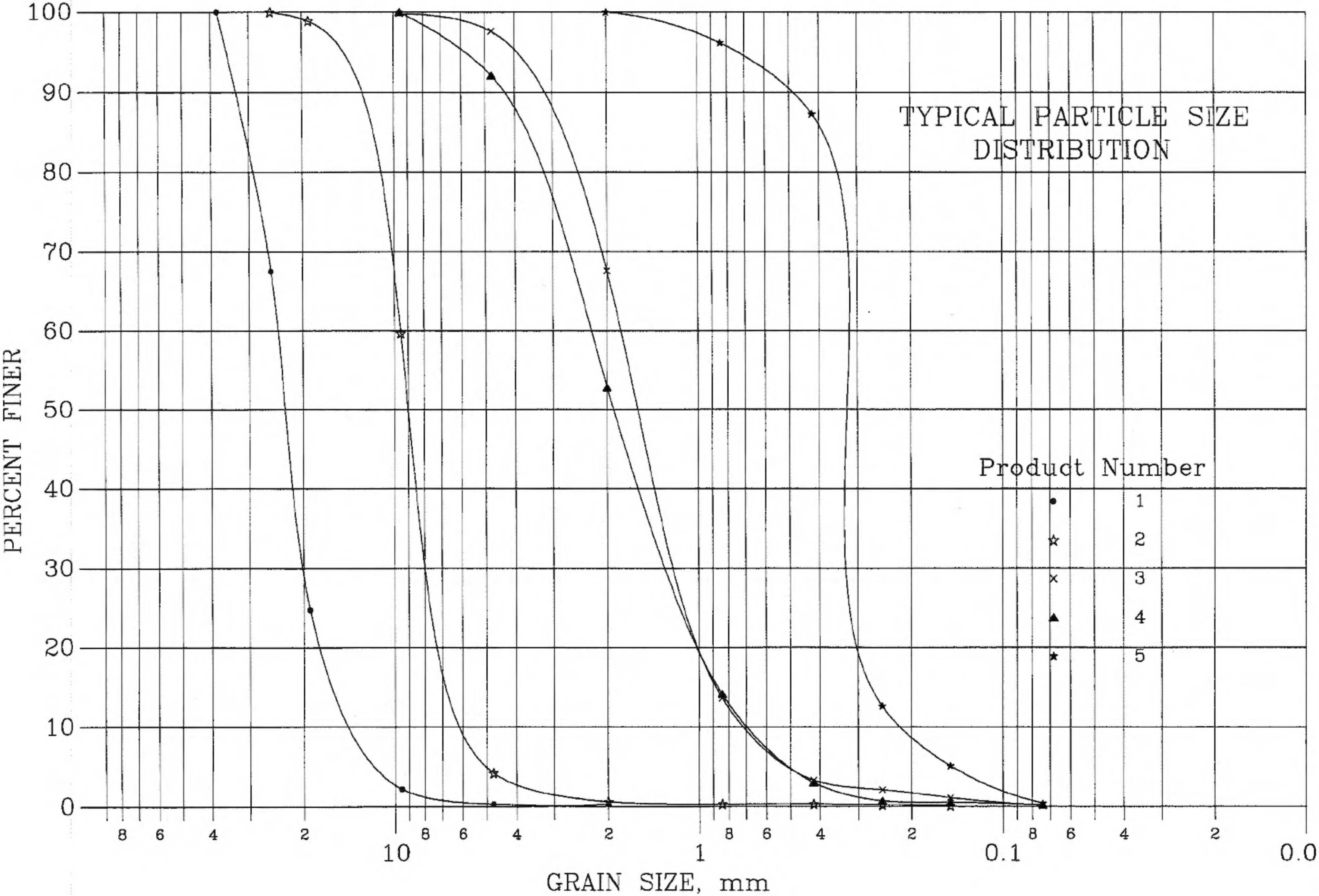

TYPICAL PARTICLE SIZE DISTRIBUTION
PERCENT FINER
100
90
80
70
60
50
40
30
20
10
0
GRAIN SIZE, mm
8 6 4 2 10 8 6 4 2 1 8 6 4 2 0.1 8 6 4 2 0.01
Product Number
1
2
3
4
5

FIGURE 1

3 consisted of stringlike pieces of rubber having an aspect ratio of approximately 1 to 16. Although all of this material passed through the 3/8 inch sieve, some particles were in excess of one inch long.

The uniformity coefficients indicate none of the materials were well graded, with all C_u values being less than 4. However, product 4 had the least uniform grain size distribution and the most random particle shape. The 5th product consisted entirely of sand sized material with all the rubber passing the No. 10 sieve and retained on the No. 200 sieve. It was the least well graded material tested.

Tests were conducted without the presence of steel from steel-belted tires. The 1.5 inch minus and the 0.75 inch minus tire chunks came from shredded glass-belted tires while the finer gradations were the result of various grinding and tread buffing operations. Not only did this facilitate the testing operation, but it was felt that removal of the steel would more closely reflect in-situ conditions following the corrosion of the steel. Photographs depicting the relative size and shape of each of the five products are shown in the appendix.

Specific Gravity and Density

Prior to shear testing, the specific gravity and compacted density were determined for each product. Density testing was conducted using AASHTO Test Method T 99-93 (*8*) without the addition of water. A 6 inch diameter by 4.584 inch deep mold having a volume of 0.075 ft^3 was utilized. The specific gravity was obtained using AASHTO Test Method T 85-91 and T 100-93 (*8*). The results of the average of three density tests and two specific gravity tests for each product are shown in Table II.

TABLE II, Compacted Density and Specific Gravity

PRODUCT	DENSITY, pcf	SPECIFIC GRAVITY
1	37.5	1.11
2	35.8	1.08
3	31.5	1.18
4	37.4	1.18
5	33.3	1.12

SHEAR STRENGTH ANALYSIS

Apparatus

Shear strength testing was conducted using a Digital Tritest 50 Triaxial Loader manufactured by Soiltest® capable of applying test loads up to 11,200 lbf. Scrap tire specimens 4 inches in diameter by 8 inches high were fabricated to densities equivalent to 100 percent of AASHTO T 99 and placed in a 6.5 inch diameter triaxial cell. The cell was fitted with a 1000 lbf. submersible load transducer to measure axial force on the sample, a 145 psi capacity pressure transducer to track cell pressure and a linear variable differential transformer to assess axial strains. Soiltest's Autonomous Data Acquisition Unit, DataSystem 6, was interfaced with an IBM 80286 to record transducer data. Manual burette readings were taken at one minute intervals during the first 10 minutes of testing and at two minute intervals thereafter. Burette measurements were later used to determine sample volume changes to adjust calculated stresses.

Samples were consolidated using de-aired water and drained triaxial tests were performed as outlined in the following sections. All samples were tested air-dried.

Compression Loading Tests

Initial tests were conducted using conventional triaxial compression testing techniques in which the confining pressure, σ_3, was held constant throughout the test. Air dried specimens were consolidated in de-aired water under confining pressures of 5.0, 6.5 and 8.0 psi. This was an effort to simulate field conditions equivalent to 4 feet of conventional fill overlying 5, 10, and 15 feet of tire chips, respectively. Confining pressures were increased in 1.0 psi increments until full consolidation pressure was realized. Burette readings were taken throughout each increment to determine when sample volume had stabilized and to assess compressibility characteristics of each product. Once the consolidation stage had been completed, vertical loading was initiated until failure was achieved or the capacity of the testing apparatus was reached.

Testing was conducted at a vertical strain rate of 0.02 in./min. Throughout the test, measurements of the applied load, vertical displacement of the specimen and volume change in the cell were taken. From these data, deviator stress, axial strain, volumetric strain, radial strain and elastic parameters of the five products could be determined.

Due to the compressible nature of the material, the limit of the vertical travel in the test apparatus was realized before the stress-strain curve deviated from a linear relationship. As a result of this phenomenon, shear failure in the traditional sense, application of a maximum deviator stress, was not attained in the compression loading series of tests.

Compression Unloading Tests

In problems involving stability of retaining walls, a decrease in lateral pressure is the stress change which leads to failure. With this in mind and desiring to obtain a real ϕ for slope stability analysis, a second series of tests was initiated in which the axial stress, σ_1, was kept constant throughout the test. In this procedure, the confining pressure was reduced from the initial consolidation pressure of 5.0, 6.5 or 8.0 psi until a shear failure in the specimen was achieved or the capacity of the test apparatus was reached. Initial tests were performed with a loading rate of 0.02 in./min. but a pore pressure build up in the samples caused premature failure. The loading rate was subsequently reduced to 0.01 in./min.

During loading, the volume change inside the cell was determined with burette measurements. To maintain a constant σ_1 the burette readings and axial displacement measurements were used to calculate changes in sample volume and area so that the appropriate decrease in cell pressure could be determined at each load increment. The area at any stage in the test, A, was calculated from the sample area, A_o, and volume, V_o, taken immediately prior to the shear stage, and the axial strain, ε_1, and volume change, ΔV, as presented by Bishop and Henkel (*9*)

$$A = A_o\ (1 + \Delta V/V_o)/(1 - \varepsilon_1)$$

Results

Compressibility

Burette readings taken throughout the consolidation phase of each triaxial series were used to calculate sample volume changes. From these data, volumetric strains, ε_v, for each product were determined as follows

$$\varepsilon_v = V_c/V_o$$

where

V_o = initial sample volume
V_c = sample volume at consolidation increment.

A plot showing percent volume change versus consolidation pressure for each material is given in Figure 2.

The consolidation behavior of all five of the products tested was essentially the same, with product 2 being the most compressible. At a confining pressure of 8.0 psi, products 1,3,4 and 5 exhibited a 27% change in volume while product 2 underwent a 32% volume change. At this confining pressure, compacted densities would increase as shown in Table III.

Table III, Density after 8.0 psi Consolidation

PRODUCT	Density at 100% T 99, pcf	DENSITY AT 8.0 psi σ_3, pcf
1	37.5	47.6
2	35.8	47.3
3	31.5	40.0
4	37.4	47.5
5	33.3	42.3

In general, there does not appear to be a correlation between particle size, shape or distribution and density or compressibility. Product 3, the material with the most elongated shape, had the least compacted unit weight but exhibited no greater tendency to consolidate than the other four materials. This is consistent with work done by Ahmed (*10*) who found very little variation in vertical strain at different stress levels in chips varying from 0.5 to 2 inches in size.

From a design and construction standpoint, the implications are that the unit weights used for settlement computations, slope stability analysis, lateral earth pressure computations and to determine fill quantities should be increased to account for the compressibility of this material.

As stated earlier, an 8.0 psi confining pressure was intended to model 4 feet of conventional fill overlying 15 feet of tire chips. It was felt that due to potential problems in generating enough processed scrap tires at any one time, construction of a fill greater than a depth of 15 feet was not realistic. Therefore, 8.0 psi would be a conservative value when evaluating the compressibility of these materials and it would appear that a unit weight of 50 pcf would be appropriate for design. This value is consistent with the results of field testing conducted in Oregon where average densities after one year of consolidation were 53 pcf (*11*).

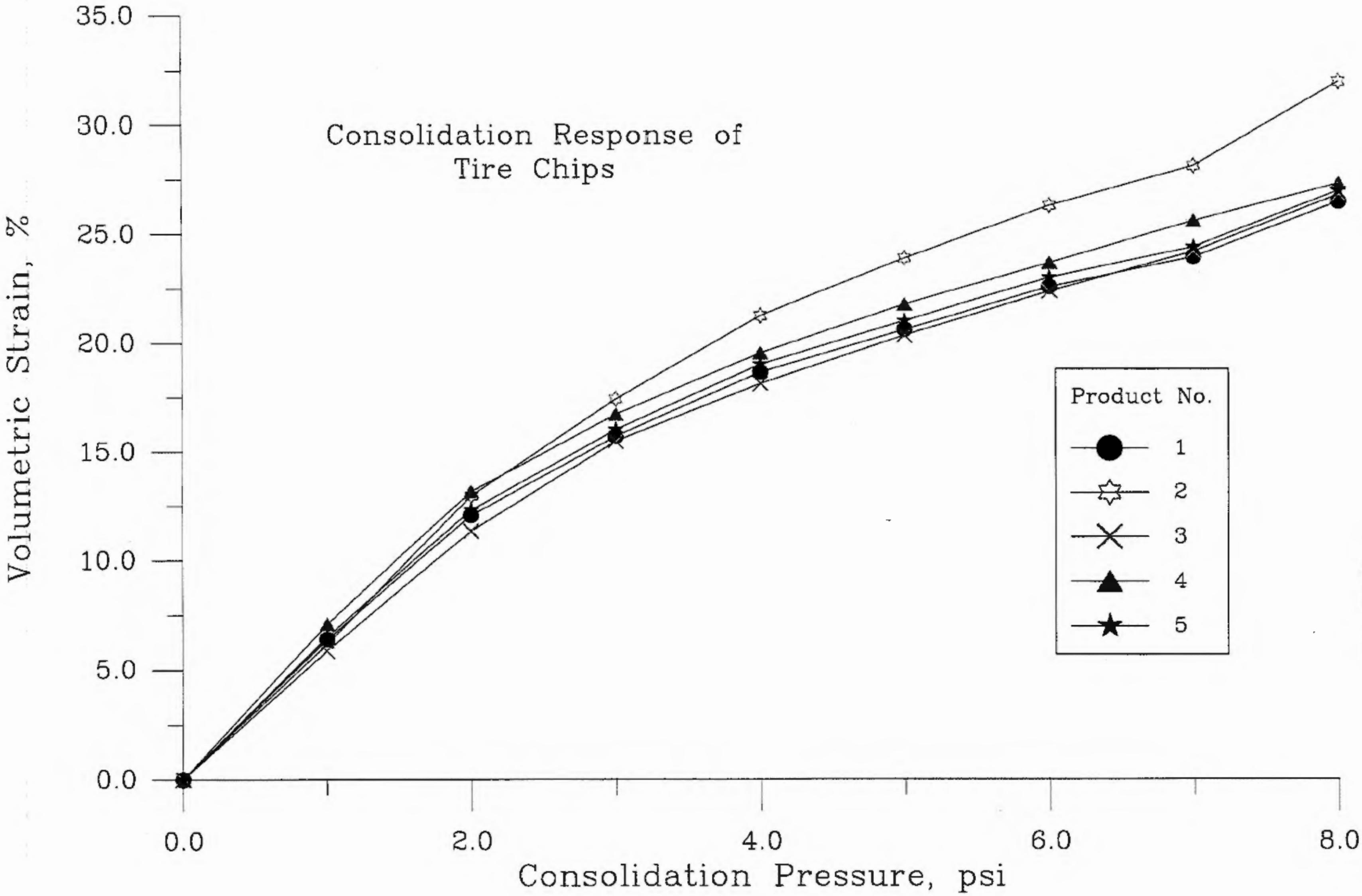
Consolidation Response of
Tire Chips
Volumetric Strain, %
Consolidation Pressure, psi
35.0
30.0
25.0
20.0
15.0
10.0
5.0
0.0
0.0
2.0
4.0
6.0
8.0
Product No.
1
2
3
4
5

Figure 2

Elastic Behavior

During each series of triaxial tests, compression loading and compression unloading, axial displacements and volume change measurements were taken. These data were then used to determine axial strains, ε_1, and volumetric strains, ε_v, in the specimens. A typical plot of deviator stress, $\sigma_1-\sigma_3$, versus axial strain and volumetric strain versus axial strain, for the constant σ_3 and constant σ_1 tests for Product 4, are shown in Figures 3 and 4, respectively. The increase in deviator stress is linear with increasing strains in the constant σ_3 series for all products tested. There is an increase in deviator stress at a given strain with increasing confining pressures for both test series. No shear plane was observed during the constant σ_1 tests but a significant amount of lateral bulge occurred at failure.

Using the information for volumetric strain and axial strain derived above, lateral strains, ε_3, in the specimens could be calculated using the relationship for triaxial loading conditions (*12*).

$$\varepsilon_3 = (\varepsilon_v - \varepsilon_1)/2$$

The data gathered from the compression loading series of tests were used to determine Poisson's ratio, μ, from which at rest earth pressure coefficients, K_o, could be determined. The following expressions were used to calculate Poisson's ratio and at rest earth pressure coefficients (*13*):

$$\mu = \varepsilon_3/\varepsilon_1$$

$$K_o = \mu/(1-\mu)$$

Young's modulus, E, was determined from the linear portion of the stress strain curves for the compression loading tests. The deviator stress at 12% strain was used in the calculation. Values of Poisson's ratio and at rest earth pressure coefficients at axial strains of 5, 10 and 15 percent, along with Young's modulus for each product at the three confining pressures used during the tests, are given in Table IV.

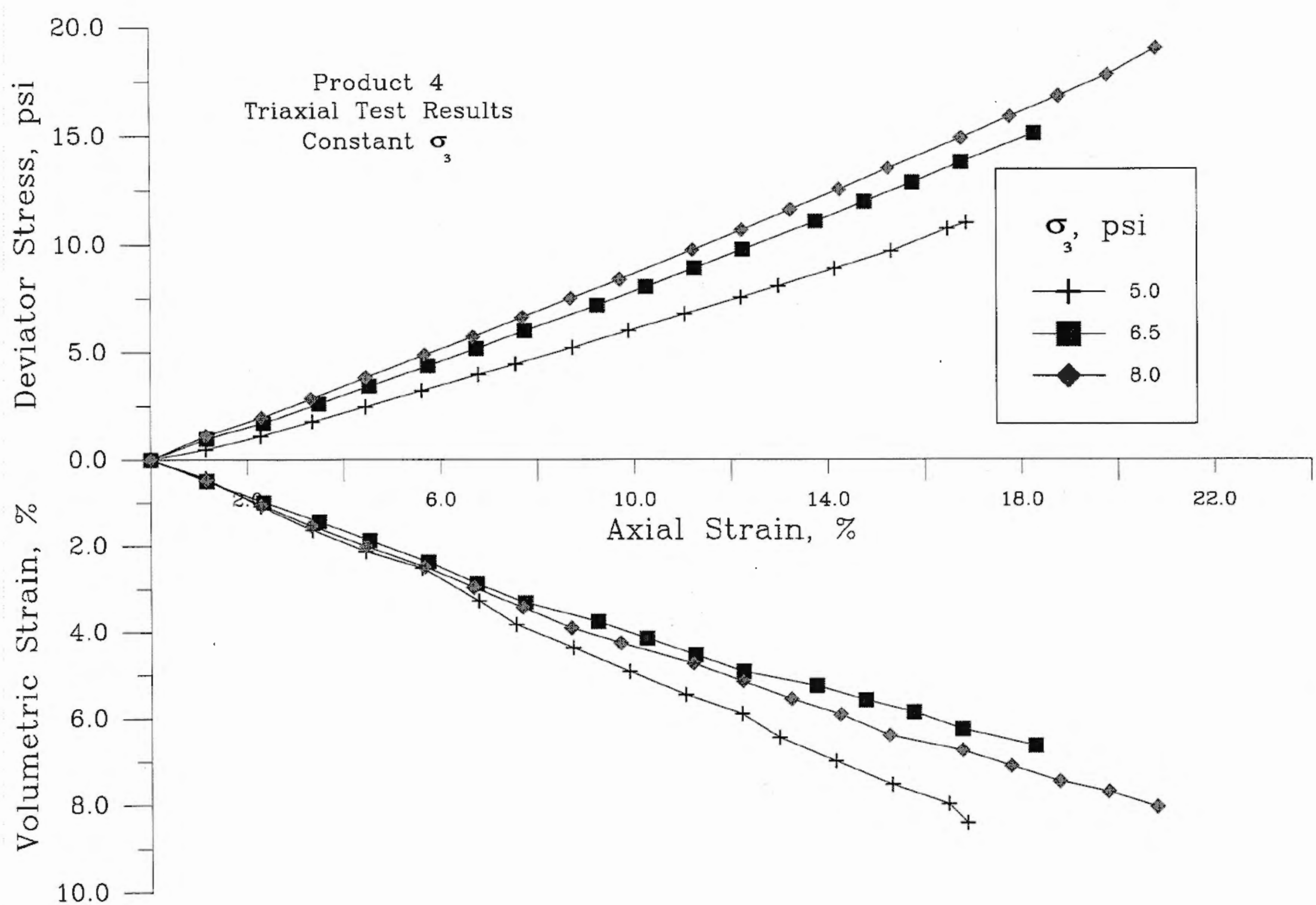
Product 4
Triaxial Test Results
Constant σ_3
Deviator Stress, psi
Volumetric Strain, %
Axial Strain, %
σ_3, psi
5.0
6.5
8.0
20.0
15.0
10.0
5.0
0.0
2.0
4.0
6.0
8.0
10.0
2.0
6.0
10.0
14.0
18.0
22.0

Figure 3

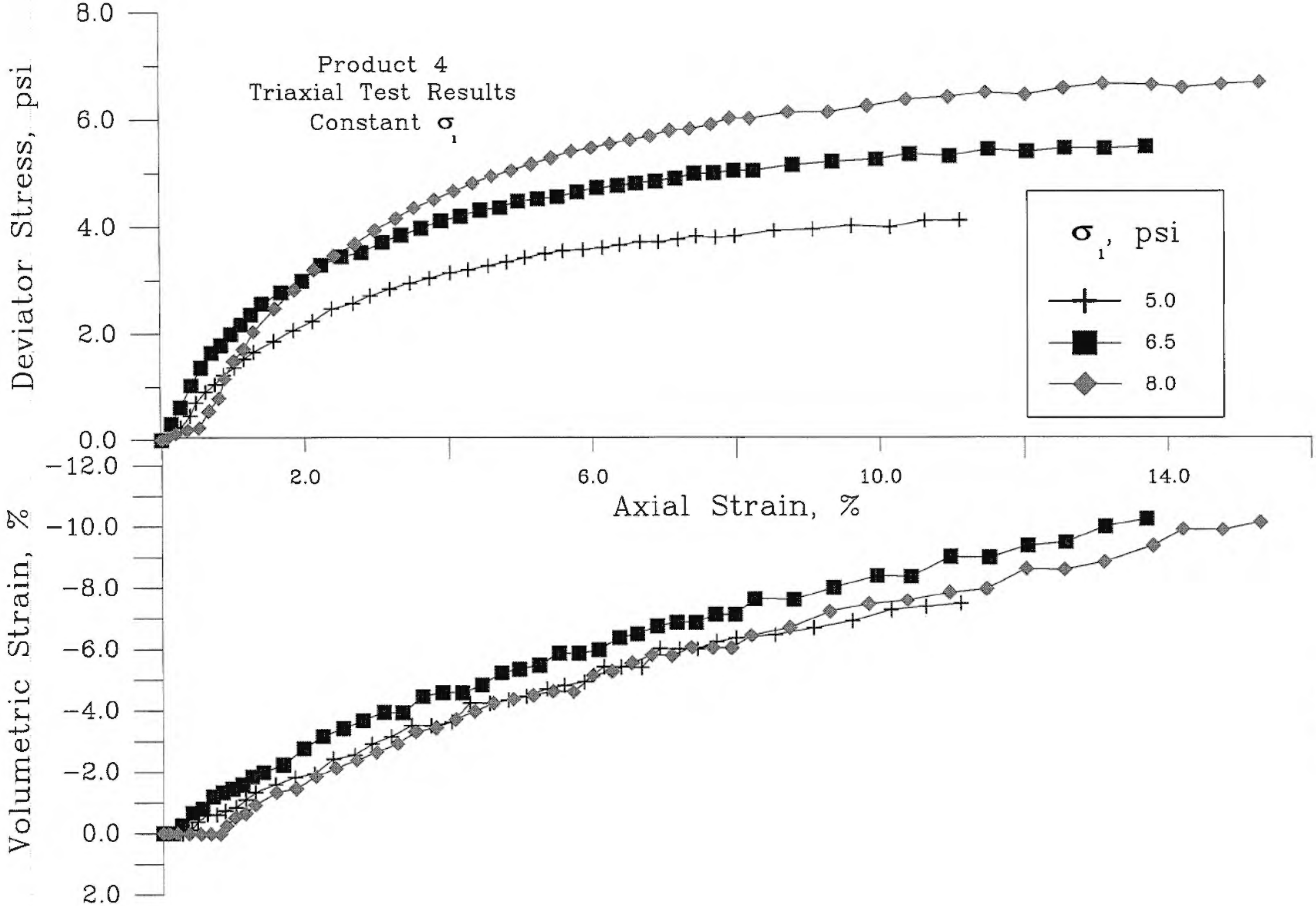

Product 4
Triaxial Test Results
Constant σ_1
Deviator Stress, psi
8.0
6.0
4.0
2.0
0.0
Axial Strain, %
2.0
6.0
10.0
14.0
Volumetric Strain, %
-12.0
-10.0
-8.0
-6.0
-4.0
-2.0
0.0
2.0
σ_1, psi
5.0
6.5
8.0

Figure 4

TABLE IV, Elastic Parameters

Product No.	σ_3 psi	μ ε_1=5%	μ 10%	μ 15%	K_o ε_1=5%	K_o 10%	K_o 15%	E psi
1	5.0	0.33	0.33	0.33	0.50	0.49	0.49	84
	6.5	0.32	0.33	0.32	0.47	0.49	0.48	85
	8.0	0.33	0.33	0.33	0.50	0.48	0.48	100
2	5.0	0.23	0.27	0.28	0.30	0.37	0.39	62
	6.5	0.31	0.31	-(1)	0.45	0.44	-(1)	70
	8.0	0.23	0.23	0.26	0.31	0.31	0.37	85
3	5.0	0.26	0.25	0.25	0.36	0.32	0.33	50
	6.5	0.24	0.25	0.26	0.31	0.33	0.34	50
	8.0	0.27	0.27	0.27	0.36	0.36	0.37	70
4	5.0	0.27	0.25	0.26	0.37	0.34	0.34	66
	6.5	0.29	0.30	0.31	0.41	0.42	0.45	79
	8.0	0.28	0.29	0.29	0.37	0.38	0.40	88
5	5.0	0.26	0.30	-(1)	0.36	0.42	-(1)	66
	6.5	0.25	0.26	-(1)	0.33	0.35	-(1)	96
	8.0	0.30	0.32	-(1)	0.36	0.42	-(1)	119

(1) Test terminated before 15% axial strain was reached.

For a given material, Poisson's ratios were relatively unaffected by changes in confining pressures and axial strain. Poisson's ratios ranged from a low of 0.23 for product 2 to a high of 0.33 for product 1. At rest earth pressure coefficients ranged from 0.30 to 0.50 which is consistent with the results of other research on processed scrap tires (*6*).

Shear Strength

A total of 31 triaxial tests were conducted to determine the shear strength of the 5 products. Initially, conventional drained tests were run in which the confining pressure, σ_3, was held constant and the vertical stress, σ_1, was increased until the strain capacity of the testing apparatus was reached. In this series of tests, the stress paths shown in the p-q plots in

Figures 5 through 9 were generated with p and q as defined by Lambe (*14*), where:

$$p = 0.5(\sigma_1 + \sigma_3)$$

and

$$q = 0.5(\sigma_1 - \sigma_3)$$

Using a K_o value of 0.40 (midway in the range determined above), and recalling that

$$K_o = \sigma_3/\sigma_1,$$

a corresponding friction angle, ϕ, of 25.4 degrees was calculated using the following relationships (*14*):

$$\sin \phi = \tan \alpha$$

and

$$q = p \tan \alpha$$

Also given in these figures are contours depicting K_o, vertical strains and the failure envelope at various friction angles. It is important to note at this point that failure was not attained in any of these tests in the conventional sense that a peak deviator stress was reached. The strain capacity of the test apparatus was realized in all cases.

A minimum failure envelope of 30 degrees was reached in the compression loading tests for each of the five products. A vertical strain of 15 to 18 percent was necessary to mobilize this friction angle. The 30 degree value is not consistent with the results of tests conducted by others in which the range of friction angles obtained was between 14 and 26 degrees (*10*). It is, however, supported by field observations of the material and K_o values obtained in this and other research (*6*).

Concern over these inconsistencies lead to the initiation of the compression unloading series of experiments. Prior to beginning the shear stage of the tests, the specimens were brought to an initial confining pressure, σ_3. Once consolidation was complete, a constant vertical stress, σ_1, was applied to the sample while the confining pressure was decreased. The cell pressure was continuously reduced until sample failure, more closely simulating the loading conditions found in a retaining wall application.

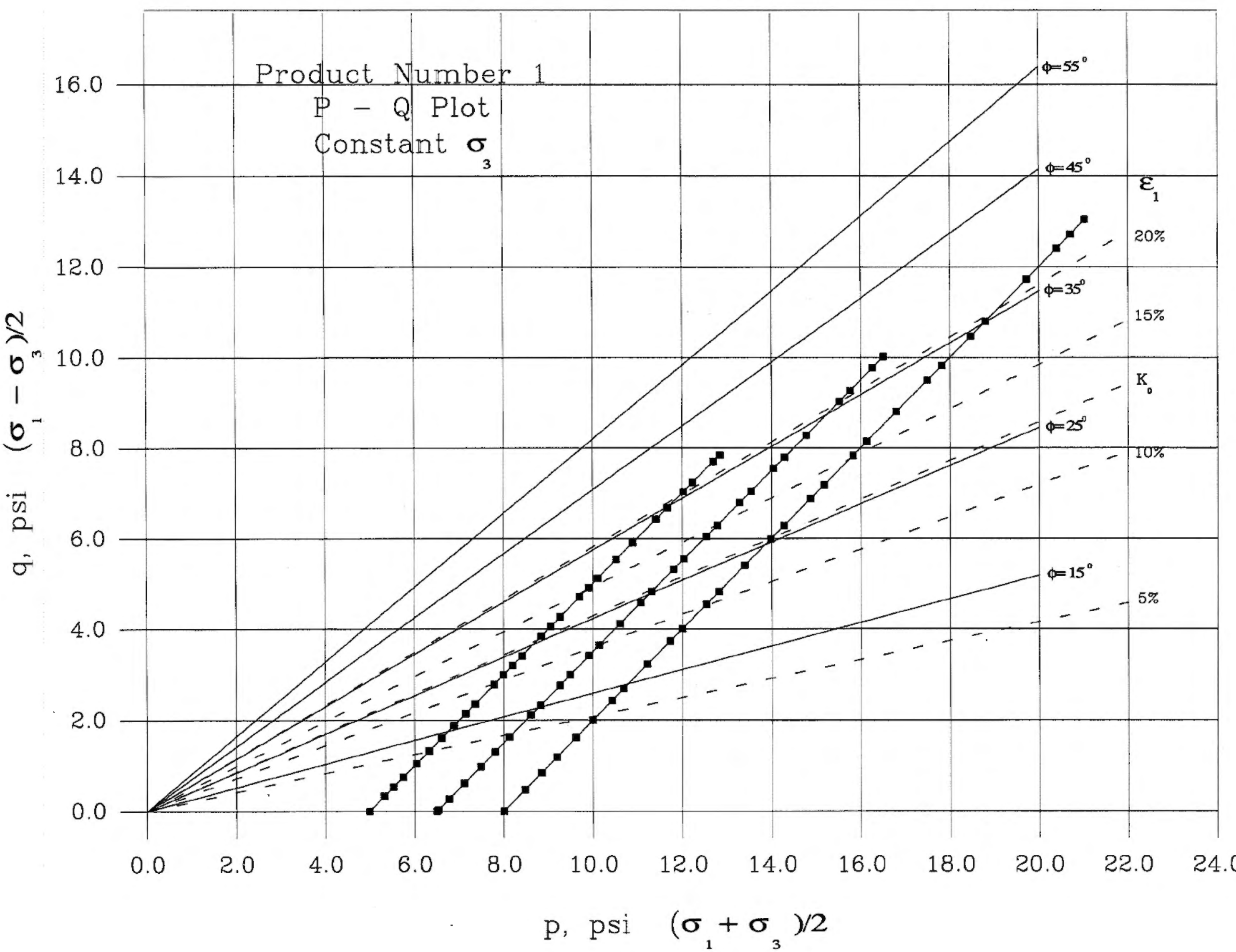
Product Number 1
P – Q Plot
Constant σ_3
q, psi $(\sigma_1 - \sigma_3)/2$
p, psi $(\sigma_1 + \sigma_3)/2$
ϕ=55°
ϕ=45°
ϕ=35°
ϕ=25°
ϕ=15°
ε_1
20%
15%
K_o
10%
5%
0.0
2.0
4.0
6.0
8.0
10.0
12.0
14.0
16.0
18.0
20.0
22.0
24.0

Figure 5

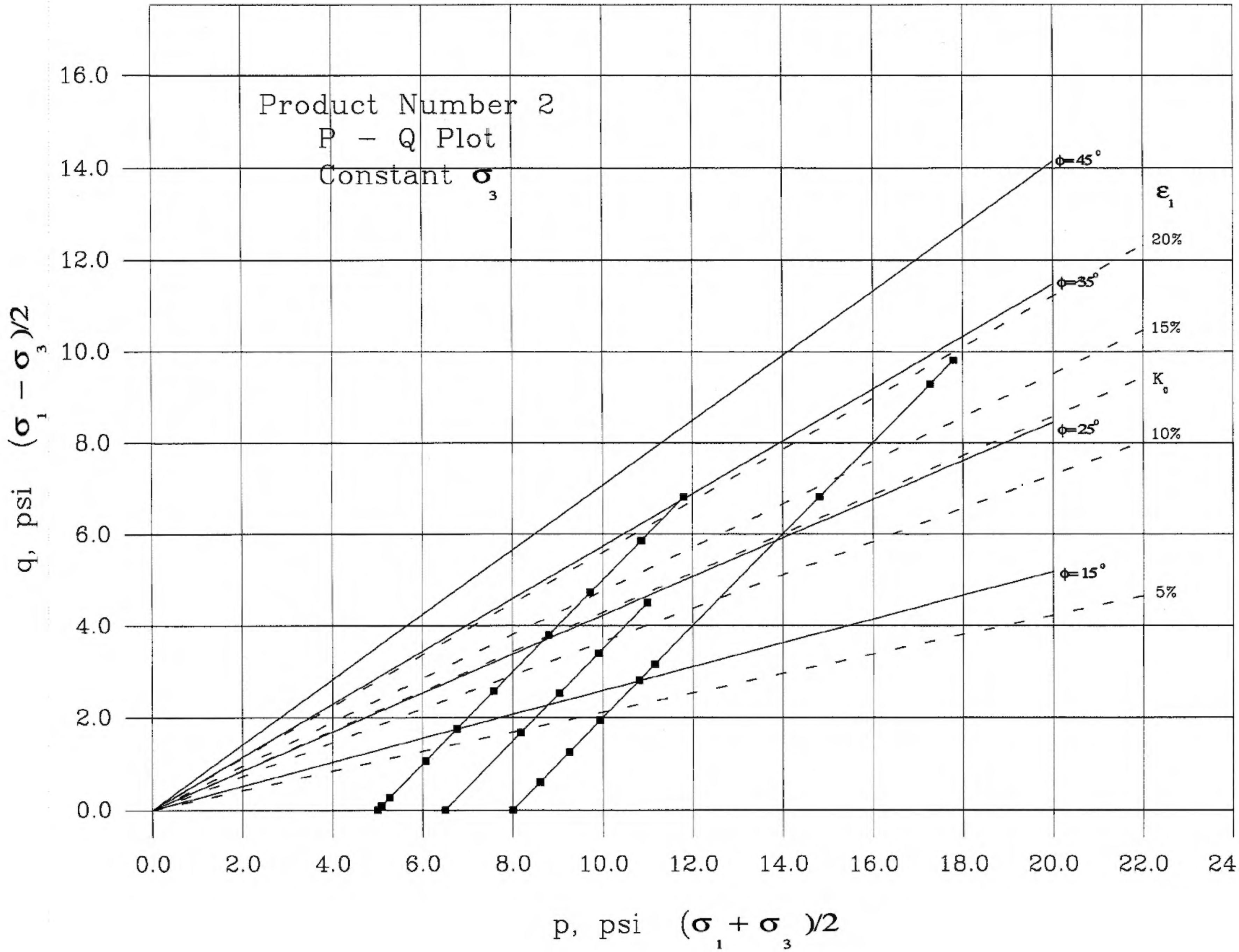
Product Number 2
P – Q Plot
Constant σ_3
q, psi $(\sigma_1 - \sigma_3)/2$
p, psi $(\sigma_1 + \sigma_3)/2$
16.0
14.0
12.0
10.0
8.0
6.0
4.0
2.0
0.0
0.0
2.0
4.0
6.0
8.0
10.0
12.0
14.0
16.0
18.0
20.0
22.0
24.0
ϕ=45°
ϕ=35°
ϕ=25°
ϕ=15°
ε_1
20%
15%
K_0
10%
5%

Figure 6

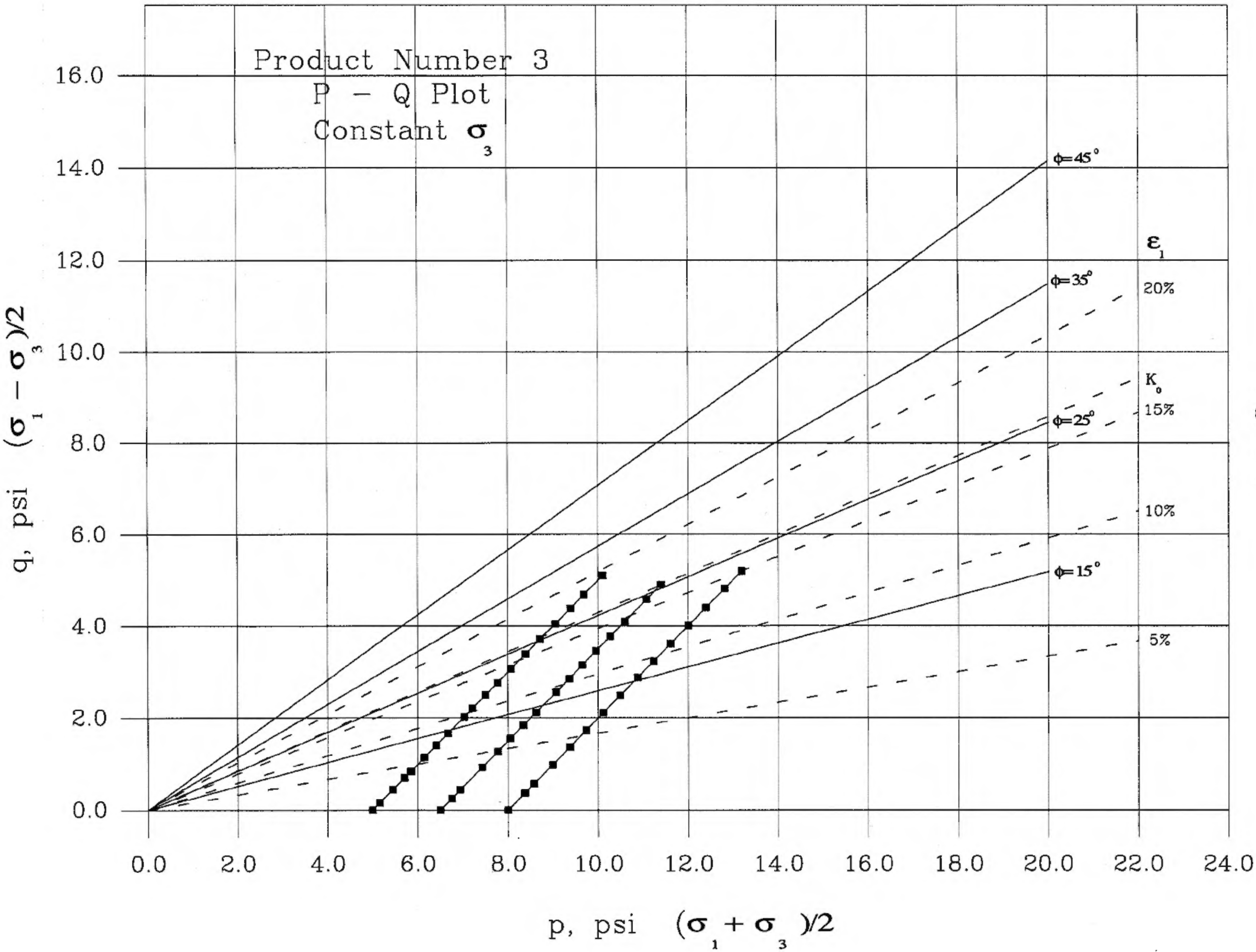
Product Number 3
P – Q Plot
Constant σ_3
ϕ=45°
ϕ=35°
ϕ=25°
ϕ=15°
ε_1
20%
K_o
15%
10%
5%
16.0
14.0
12.0
10.0
8.0
6.0
4.0
2.0
0.0
q, psi $(\sigma_1 - \sigma_3)/2$
0.0
2.0
4.0
6.0
8.0
10.0
12.0
14.0
16.0
18.0
20.0
22.0
24.0
p, psi $(\sigma_1 + \sigma_3)/2$

Figure 7

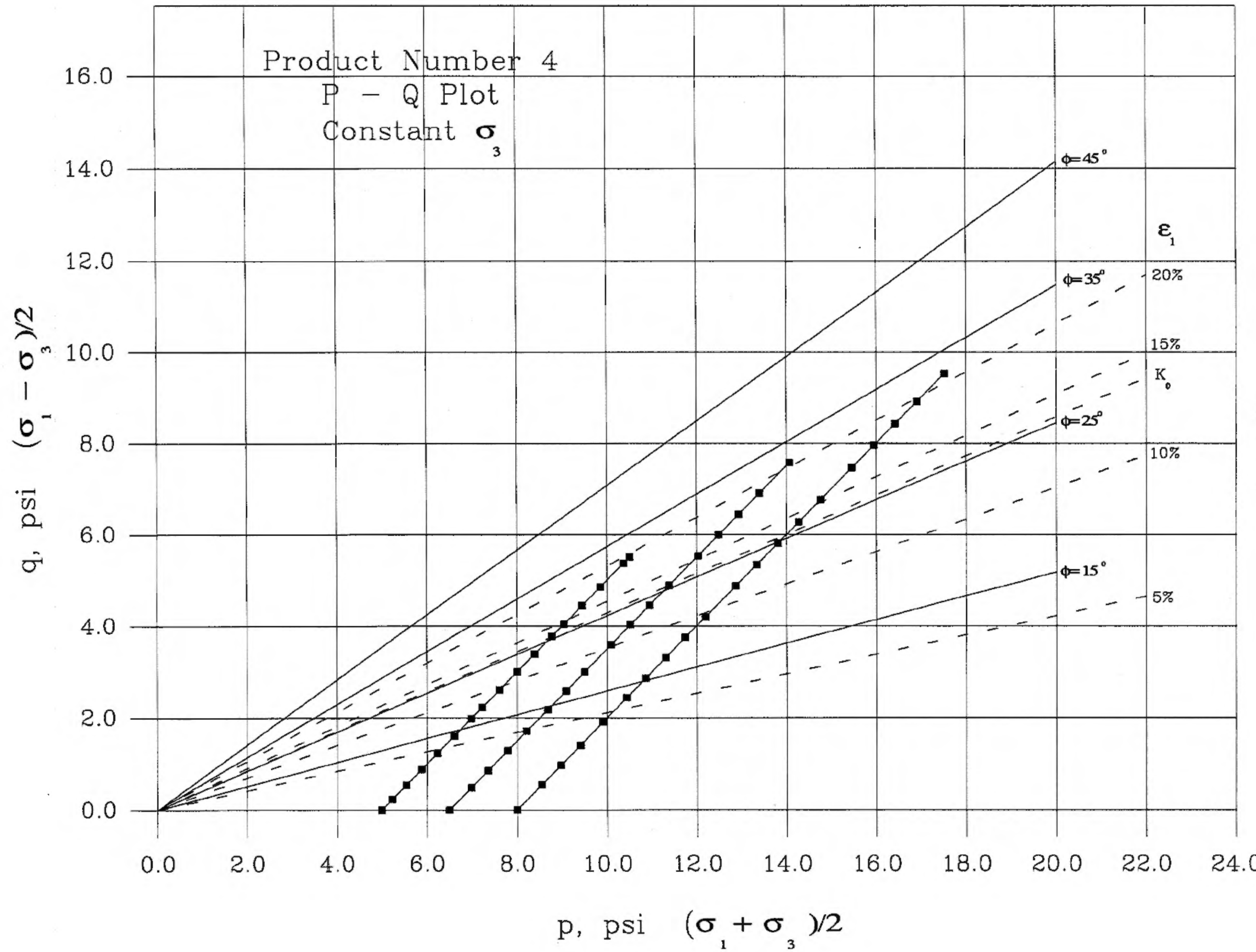

Product Number 4
P – Q Plot
Constant σ_3
q, psi $(\sigma_1 - \sigma_3)/2$
p, psi $(\sigma_1 + \sigma_3)/2$
$\phi=45°$
$\phi=35°$
$\phi=25°$
$\phi=15°$
ε_1
20%
15%
K_0
10%
5%

Figure 8

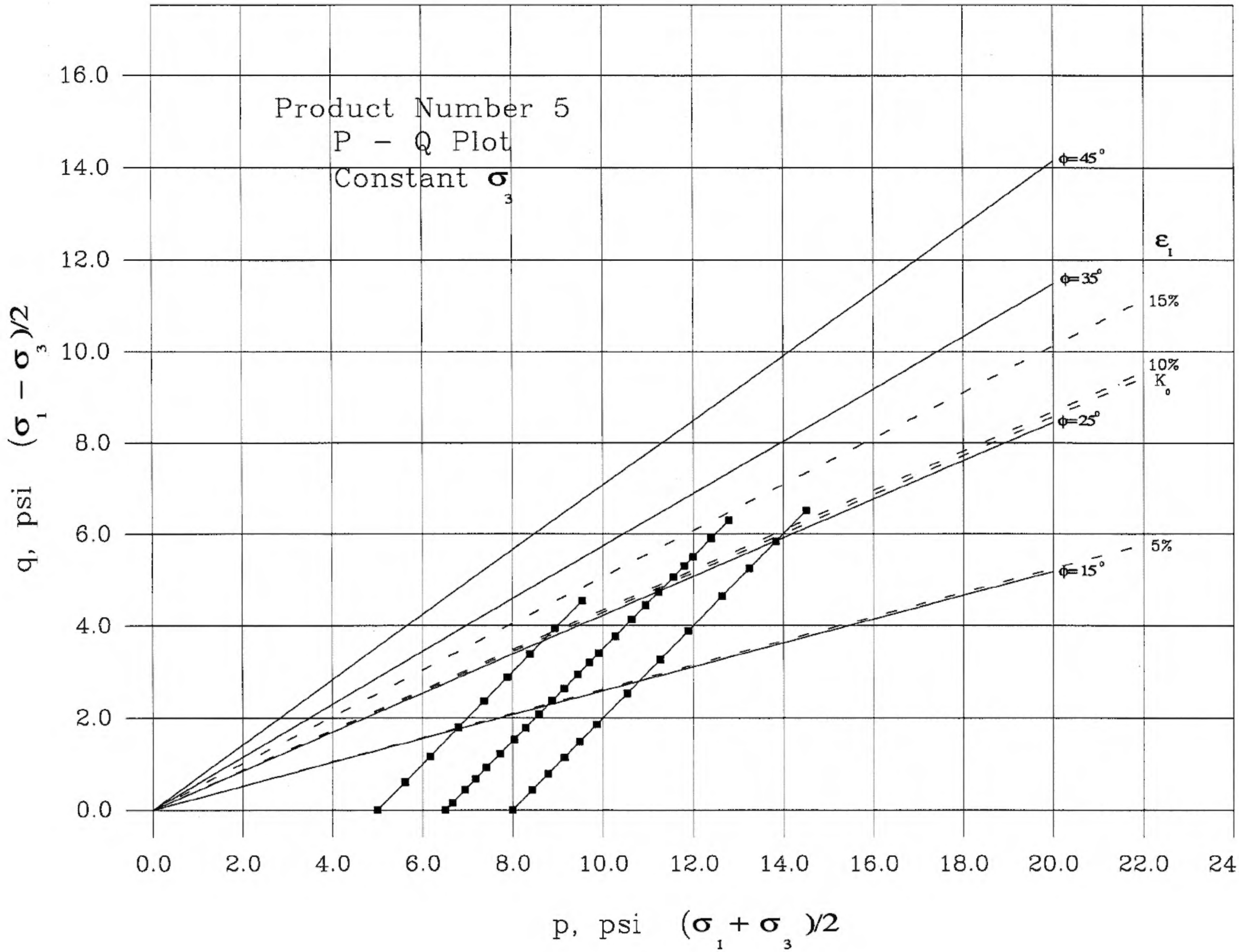
Product Number 5
P – Q Plot
Constant σ_3
q, psi $(\sigma_1 - \sigma_3)/2$
p, psi $(\sigma_1 + \sigma_3)/2$
ϕ=45°
ϕ=35°
ϕ=25°
ϕ=15°
ε_1
15%
10%
K_0
5%
16.0
14.0
12.0
10.0
8.0
6.0
4.0
2.0
0.0
0.0
2.0
4.0
6.0
8.0
10.0
12.0
14.0
16.0
18.0
20.0
22.0
24.0

Figure 9

Presented in Figures 10 through 14 are the P-Q plots for the compression unloading series of triaxial tests. These graphs give the stress paths followed during the test, the failure envelope at various friction angles and contours of lateral strains, ε_3, for each product.

For the two larger particle distributions, failure occurred at a lateral strain of approximately 10 percent while the smaller size materials failed at lower strain levels. Friction angles obtained from this set of tests ranged from a low of 45 degrees for product 4 to a high of 60 degrees for product 3. As with the compression loading tests, the peak friction angle for the 1.5 inch size material was slightly higher than for the 0.75 inch material. Although these peak values could be used in embankment design, they would not be appropriate for retaining wall analysis. In order to fully mobilize this strength behind a retaining wall, an unacceptable amount of lateral movement would need to occur. For retaining wall design, a friction angle between 25 and 30 degrees, corresponding to lateral strains between at rest conditions and 1 percent lateral strain, would be appropriate.

A summary of friction angles obtained form each series of tests is given in Table V.

TABLE V, Shear Strength

Values of ϕ, degrees

		Constant σ_3			Constant σ_1		
		ε_1			ε_3		
PRODUCT	SIZE	10%	15%	20%	1%	5%	10%
1	1.5"	21.1	29.5	35.5	32.6	48.5	57.0
2	0.75"	21.4	28.4	34.1	29.1	44.0	52.3
3	0.375"	17.2	23.2	31.2	30.1	47.0	-
4	0.375"	20.6	27.0	32.1	29.8	42.7	-
5	No. 10	25.8	30.4	-	30.1	41.8	-

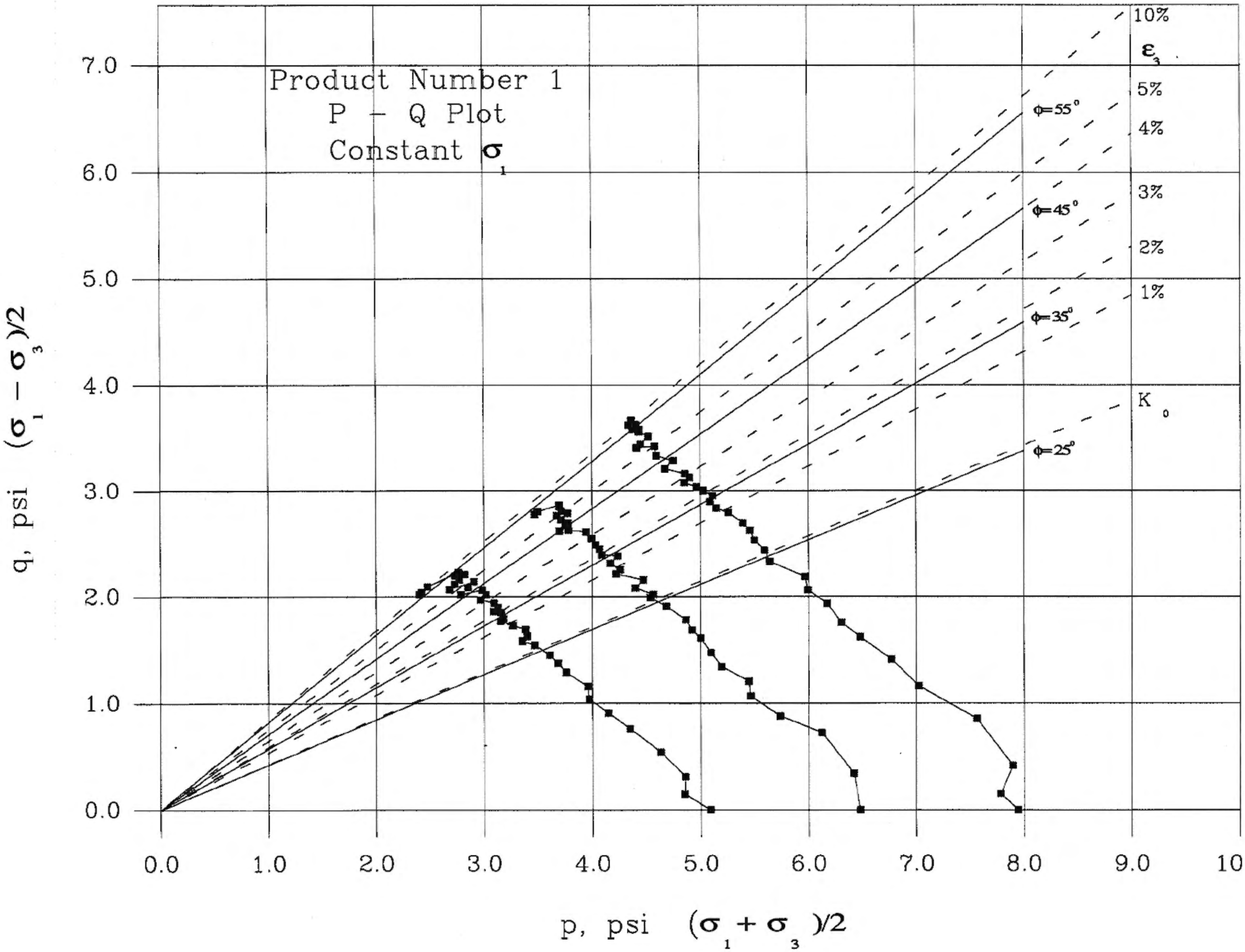

Product Number 1
P – Q Plot
Constant σ_1
q, psi $(\sigma_1 - \sigma_3)/2$
p, psi $(\sigma_1 + \sigma_3)/2$
0.0
1.0
2.0
3.0
4.0
5.0
6.0
7.0
8.0
9.0
10.0
φ=55°
φ=45°
φ=35°
φ=25°
10%
ε_3
5%
4%
3%
2%
1%
K_0

Figure 10

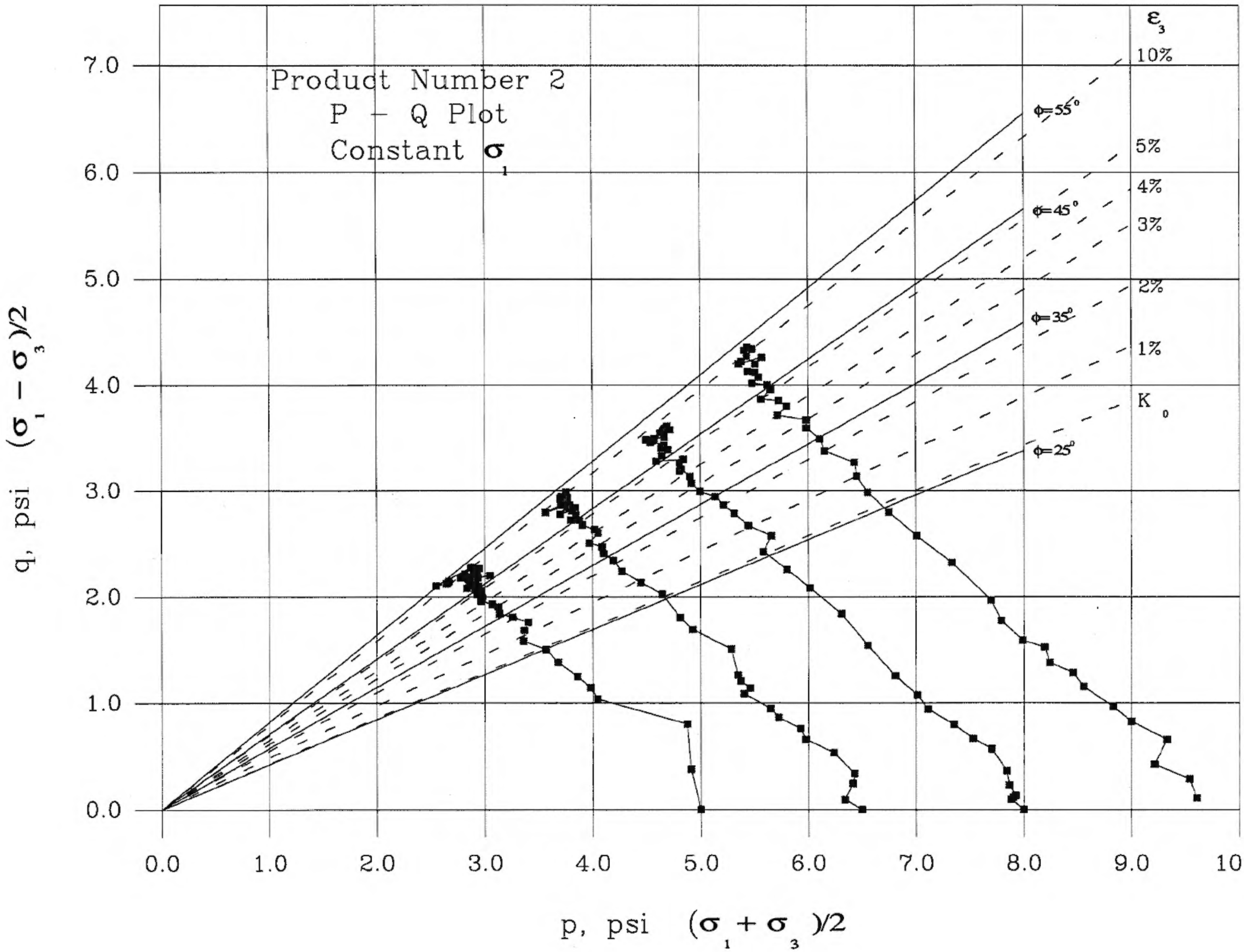

Product Number 2
P – Q Plot
Constant σ_1
ε_3
10%
5%
4%
3%
2%
1%
K_0
$\phi=55°$
$\phi=45°$
$\phi=35°$
$\phi=25°$
q, psi $(\sigma_1 - \sigma_3)/2$
p, psi $(\sigma_1 + \sigma_3)/2$
0.0
1.0
2.0
3.0
4.0
5.0
6.0
7.0
8.0
9.0
10.0

Figure 11

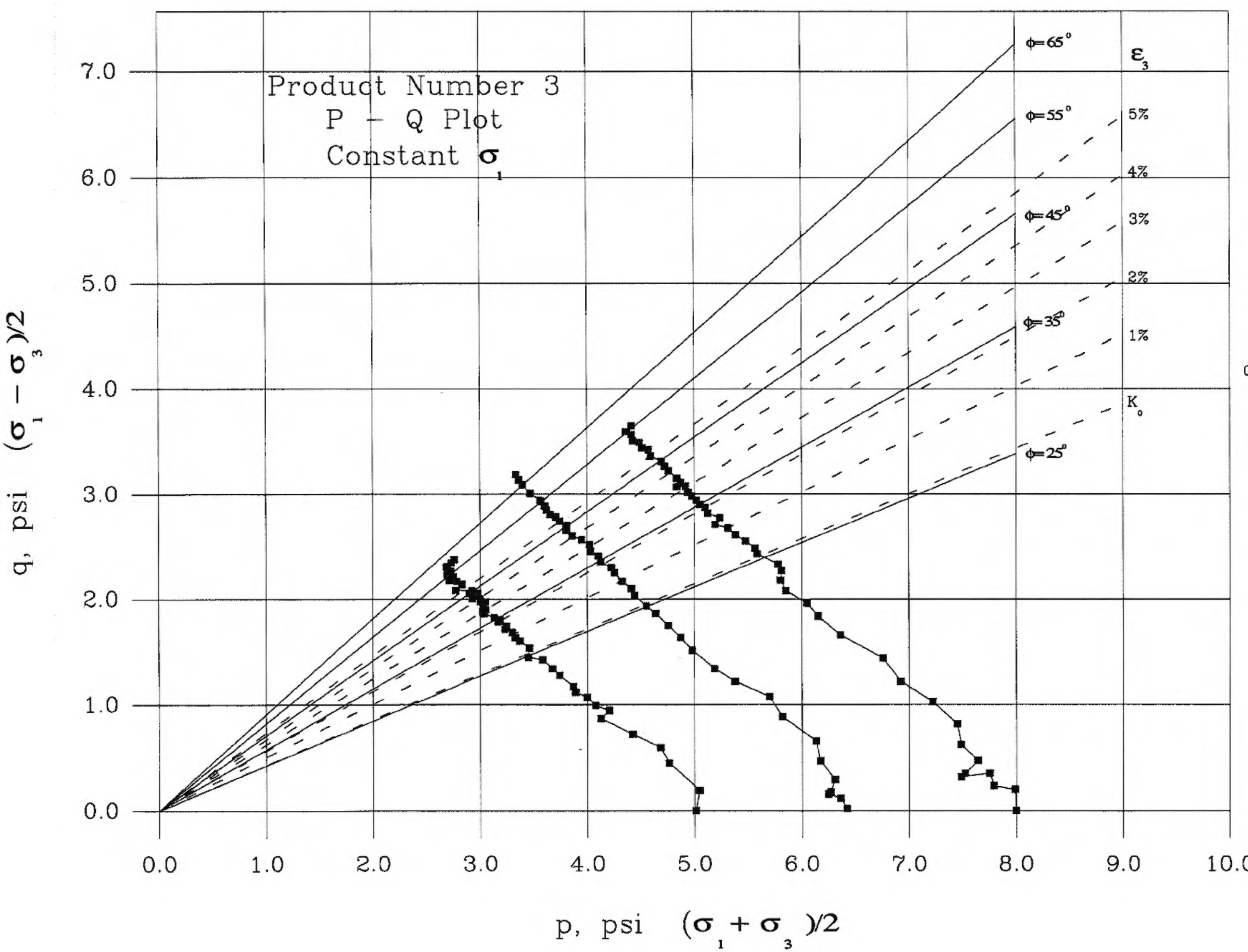

Product Number 3
P – Q Plot
Constant σ_1
q, psi $(\sigma_1 - \sigma_3)/2$
p, psi $(\sigma_1 + \sigma_3)/2$
ϕ=65°
ϕ=55°
ϕ=45°
ϕ=35°
ϕ=25°
ε_3
5%
4%
3%
2%
1%
K_o
0.0
1.0
2.0
3.0
4.0
5.0
6.0
7.0
8.0
9.0
10.0

Figure 12

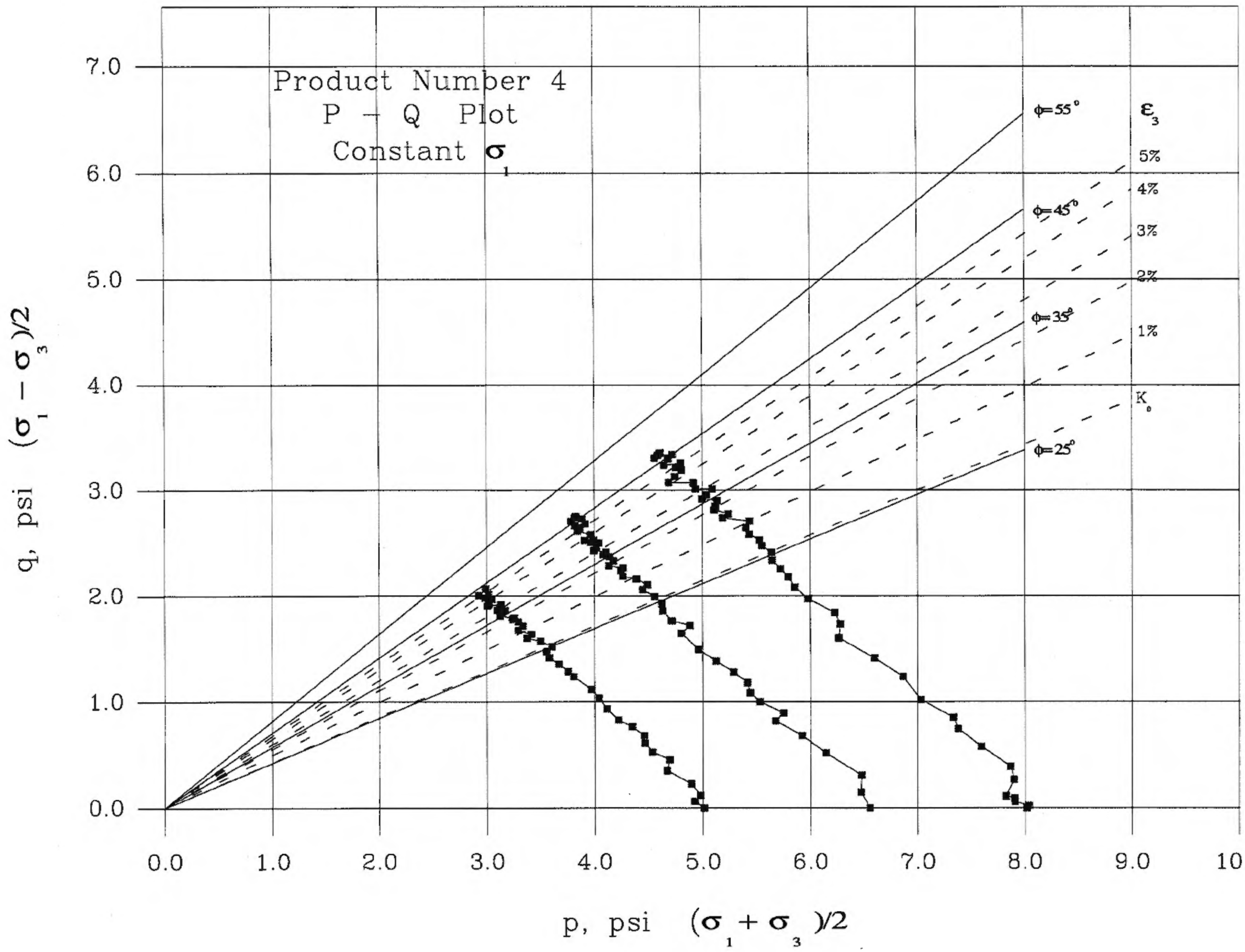
Product Number 4
P – Q Plot
Constant σ_1
ϕ=55°
ϕ=45°
ϕ=35°
ϕ=25°
ε_3
5%
4%
3%
2%
1%
K_o
q, psi $(\sigma_1 - \sigma_3)/2$
p, psi $(\sigma_1 + \sigma_3)/2$
0.0
1.0
2.0
3.0
4.0
5.0
6.0
7.0
8.0
9.0
10.0

Figure 13

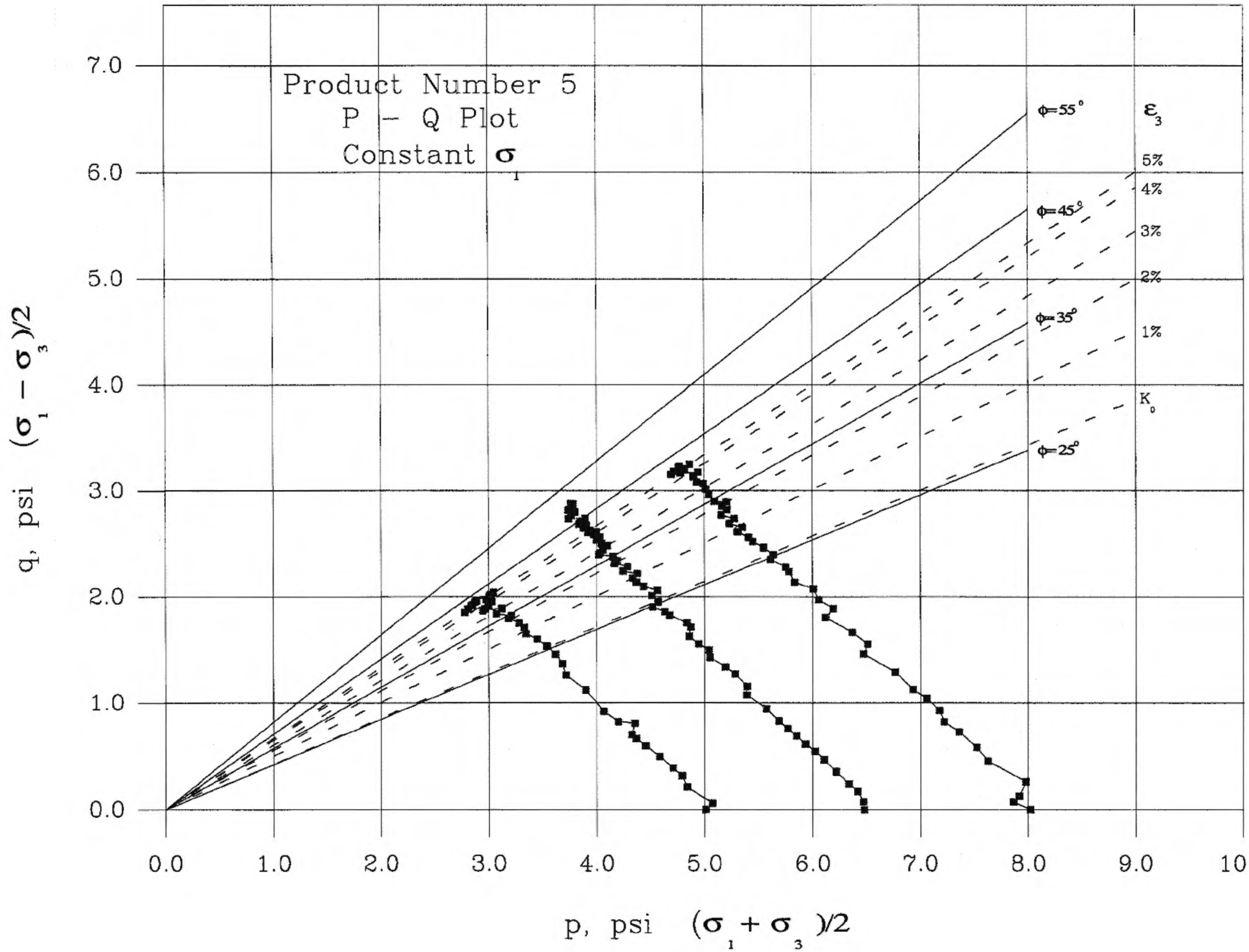
Product Number 5
P – Q Plot
Constant σ_1
ϕ=55°
ϕ=45°
ϕ=35°
ϕ=25°
ε_3
5%
4%
3%
2%
1%
K_o
q, psi $(\sigma_1 - \sigma_3)/2$
p, psi $(\sigma_1 + \sigma_3)/2$
0.0
1.0
2.0
3.0
4.0
5.0
6.0
7.0
8.0
9.0
10.0

Figure 14

CONCLUSIONS AND RECOMMENDATIONS

1. The five scrap tire products tested in this research were all found to be uniformly graded. Products 1 and 2 were chips with maximum sizes of 1.5 inches and 0.75 inches, respectively. Products 3 and 4 each had a top size of 0.375 inches but product 3 was composed of elongated, string-like particles while the shape of product 4 was more angular and random in nature. Product 5 consisted of sand size grains with 100 percent passing the No. 10 sieve.

2. Specific gravities were in the range of 1.08 to 1.18. Compacted dry densities at 100% of T 99 energy varied between 31.5 pcf for product 3 and 37.5 pcf for product 1.

3. Compressibility testing resulted in similar behavior for all five materials. At a confining pressure of 8.0 psi, the samples exhibited a 27 percent to 32 percent reduction in volume. This translates into densities of 42.3 to 47.6 pcf.

4. In general, there does not appear to be a correlation between particle size, shape or distribution and density or compressibility for the materials tested. Product 3, the material with the most elongated shape, had the least compacted density but exhibited no greater propensity for consolidation that the other four products.

5. Based on the research documented herein and work conducted by others, a unit weight of 50 pcf for is recommended for use in design when processed scrap tires are to be incorporated in walls and embankments.

6. From the compression loading series of triaxial tests, it was determined that for a given material, Poisson's ratios were relatively unaffected by changes in confining pressures and volumetric strain. Poisson's ratios ranged from a low of 0.23 for product 2 to a high of 0.33 for product 1. At rest earth pressure coefficients, K_o, varied from 0.30 to 0.50.

7. Conventional drained triaxial compression tests, in which the confining pressure, σ_3, is held constant while the axial stress, σ_1, is increased, could not be used to obtain an ultimate shear strength of these materials. The strain capacity of the testing apparatus was realized before a peak deviator stress, $\sigma_1-\sigma_3$, was attained. A minimum failure envelope of 30 degrees was reached for all products at a vertical strain of 15 to 18 percent. This is consistent with field observations and K_o values obtained in this and other research.

8. The compression unloading triaxial test, in which σ_1 is held constant and σ_3 is decreased, is a more appropriate tool for predicting the behavior of this material in slopes and behind retaining walls. For the two larger products, failure occurred at a lateral strain of approximately 10 percent while the smaller

size materials failed at lower strain levels. Peak friction angles from this set of tests ranged from a low of 45 degrees for product 4 to a high of 60 degrees for product 3.

9. It is recommended that a friction angle of 45 degrees be used for embankment design. When tire chips are used as backfill behind a retaining wall, it is suggested that an at rest coefficient of lateral earth pressure of 0.40 be used for design.

10. Additional research is recommended to further investigate the effect of gradation on the performance of tire chips and to verify the K_o value selected for design. All the products tested in this research were uniformly graded materials. It is suggested that a well graded product be fabricated using material passing the one inch sieve and retained on the No. 4 sieve. To verify that the at rest earth pressure coefficient design value of 0.40 is appropriate, triaxial tests should be run with σ_3/σ_1 equal to approximately 0.40.

ACKNOWLEDGEMENTS

The author wishes to thank Dr. Jim Olson of the University of Vermont, Department of Civil Engineering for his guidance and support throughout this research. The assistance of Nicolaas Garbacik and William Gray of the Vermont Agency of Transportation's Materials and Research Division with the experimental work is also very much appreciated.

REFERENCES

1. *Markets for Scrap Tires,* U.S. Environmental Protection Agency, Office of Solid Wastes, Oct. 1991.

2. Epps, J.A., *NCHRP Synthesis of Highway Practice 198: Uses of Recycled Rubber Tires in Highways,* TRB, National Research Council, Washington, D.C., 1994.

3. Winters, P., *Use of Tire Chips in a Highway Embankment,* Research update U91-5, Vermont Agency of Transportation, April 1991.

4. Frascoia, R.I., *Tire chips in the Base Course of a Local Road,* Report 94-2, Vermont Agency of Transportation, March 1994.

5. Humphrey, D.N., and W.P. Manion. Properties of Tire Chips for Lightweight Fill. In *Grouting, Soil Improvement and Geosynthetics* (R.H. Borden et al., eds.), ASCE, Vol. 2, 1992, pp. 1344-1355.

6. Humphrey, D.N., T.C. Sanford, M.M. Cribbs and W.P. Manion. Shear Strength and Compressibility of Tire Chips for Use as

Retaining Wall Backfill. In *Transportation Research Record 1422,* TRB National Research Council, Washington, D.C., 1993, pp. 29-35.

7. Eaton, R.A., R.J. Roberts, and D.N. Humphrey. *Gravel Road Test Sections Insulated with Scrap Tire Chips; Construction and First Year's.* Special Report 94-21, U.S. Army Corps of Engineers Cold Regions Research and Engineering Laboratory, Hanover, NH, Aug. 1994.

8. *Standard Specifications for Transportation Materials and Methods of Sampling and Testing, Part II: Methods of Sampling and Testing,* 16th ed. AASHTO, Washington, D.C., Jan. 1993.

9. Bishop, A.W., and D.J. Henkel. *The Measurement of Soil Properties in the Triaxial Test.* Edward Arnold Publishers, Ltd., London, 1957.

10. Ahmed, I., *Laboratory Study on Properties of Rubber - Soils,* Joint Highway Research, Indiana Department of Transportation-Department of Civil Engineering, Purdue University, West Lafayette, May 1993.

11. Upton, R., and G. Machan. Use of Shredded Tires for Lightweight Fill. Presented at 72nd Annual Meeting of the Transportation Research Board, Washington, D.C., Jan 1993.

12. Das, B.M. *Advanced Soil Mechanics.* Hemisphere Publishing Co., New York, 1983.

13. Wu, T.H. *Soil Mechanics.* Allyn and Bacon, Inc. Boston, Ma., 1976.

14. Lambe, T.W. Methods of Estimating Settlements. In *Journal of Geotechnical Engineering,* ASCE, Vol. 90, No. SM5, 1964, pp. 47-74.

APPENDIX

Photography by P. Pelkey and R. Frascoia

APPENDIX

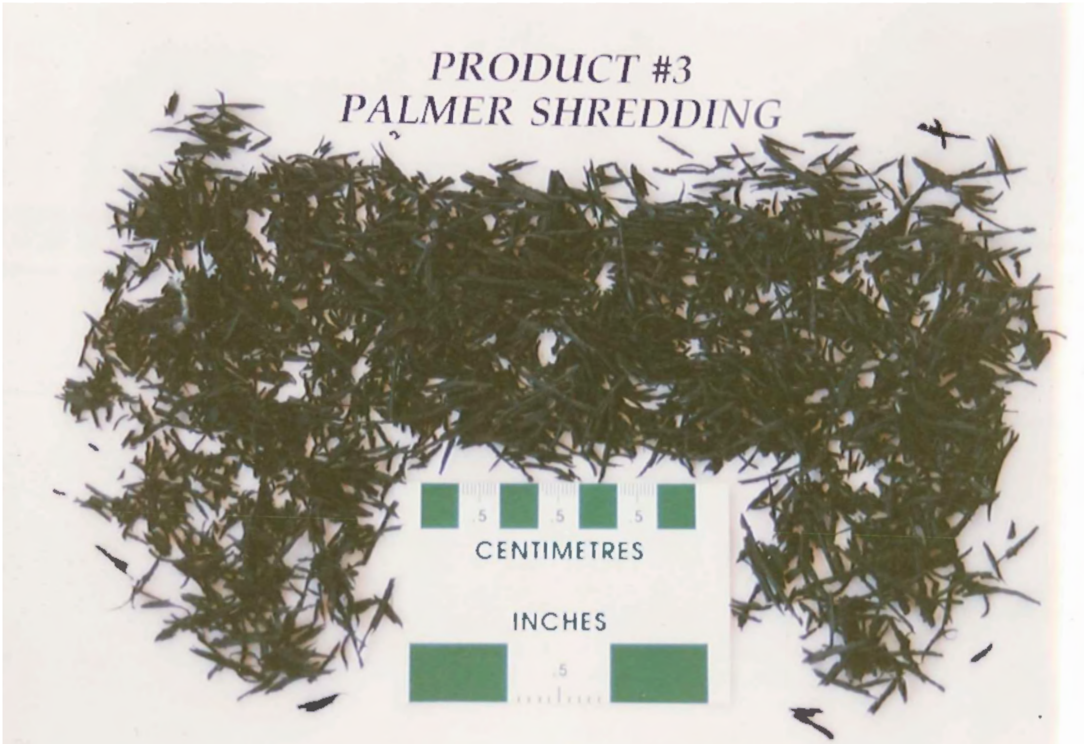

Photography by P. Pelkey and R. Frascoia

Appendix

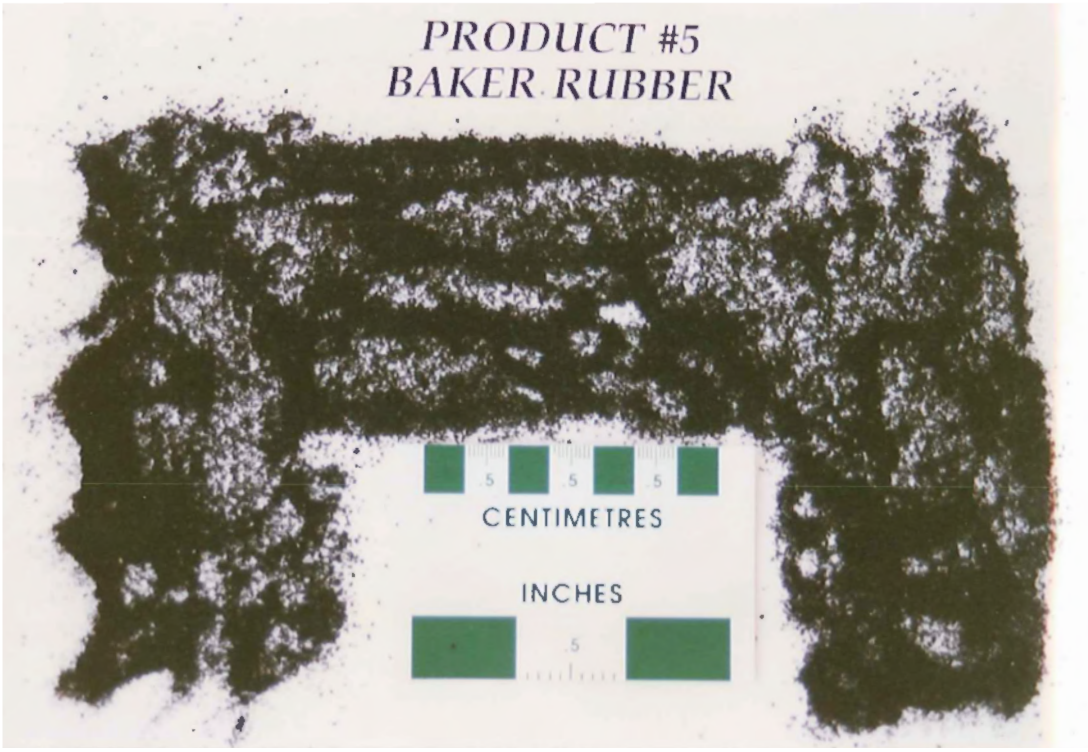

Photography by P. Pelkey and R. Frascoia